# Remarkable difference in structural relaxation dynamics of conventionally prepared bulk glass and vapor-deposited thin films

Jiri Málek[1], Roman Svoboda

*Department of Physical Chemistry, Faculty of Chemical Technology, University of Pardubice, Studentská 573 , 532 10, Czech Republic*

**ABSTRACT:** The structural relaxation dynamics of conventionally prepared bulk glass of N,N'-bis(3-methylphenyl)-N,N'-diphenyl-benzidine (TPD) was measured by Differential Scanning Calorimetry. The calorimetric data were quantitatively described in terms of the Tool-Narayanaswamy-Moynihan (TNM) model. The TNM parameters were evaluated using a combination of linearization and non-linear optimization methodologies: $h^*/R$ = 109.5 kK, ln(A/s) = -321, $\beta$ = 0.37, $x$ = 0.64. Additionally, the TNM phenomenology was used to describe recently reported normalized thickness data of stable and aged thin TPD films measured by ellipsometry. The structural relaxation was found to proceed at a markedly higher rate in these thin films prepared by the physical vapor deposition compared to that of conventional bulk glass. This feature appears to be associated with the significantly narrower distribution of relaxation times ($\beta \cong 0.8$) observed for stable thin film in 'as-deposited' form with uniquely dense molecular packing. Interestingly, very similar attributes of the relaxation kinetics were also found in the aged thin film with a previously erased thermal history associated with the deposition.

## INTRODUCTION

The *stable glasses* discovered in 2007 by Ediger and his research group[1] represent a unique class of glassy materials with high kinetic and thermal stability, as well as a customized molecular orientation. They are prepared by physical vapor deposition (PVD) at a substrate temperature controlled well below the glass transition temperature ($T_g$). Several reviews and perspectives have recently been published[2-5] discussing the main characteristics and remarkable features of stable glasses, the mechanism of their formation, and tuning their molecular packing. For instance, N,N'-bis(3-methylphenyl)-N,N'-diphenyl-benzidine (referred to as TPD) is a hole transport semiconducting material commonly used in organic light-emitting diodes that easily forms a stable high-density glass upon PVD. The molecular orientation in glassy TPD is tunable and controlled by the substrate temperature[6,7] and these materials exhibit high thermal stability and universality of transformation front behavior.[8] A unique method to probe surface diffusion of this material has been used and it was demonstrated that the surface diffusion is greatly enhanced in TPD stable glass compared to a bulk glass.[9] The long-range correlated dynamics in TPD ultra-thin molecular glass films prepared by vapor deposition at bulk $T_g$ was measured as a function of film thickness.[10] Zhang and Fakhraai[11] reported

[1] Corresponding author: jiri.malek@upce.cz

first measurement of surface diffusion on stable TPD glass, and compared with physically aged and conventionally prepared glass. They found no change in the surface diffusion coefficients when the expected structural relaxation time varied over many orders of magnitude. It was suggested that fast surface diffusion is decoupled from the bulk dynamics in TPD stable glass and is probably associated with the near-surface dynamics involving a few monolayers of top surface molecules where they can equilibrate at a short time scale.[11]

Ráfols-Ribé et al.[12] have shown that the thermal conductivity in vapor-deposited thin-film TPD glasses is anisotropic and is controlled by the deposition temperature. The stable thin-film glasses transform into the liquid state via front propagation starting at the most mobile surfaces.[8] The fast calorimetric studies have shown that once the surface mobility is arrested by capping the free surface of a stable glass the glasses transform via a homogeneous mechanism.[13] The relationship between the growth front velocity and the stability of the glass is explained through the existence of an ultrathin intermediate layer at the interface of the moving front with a lifetime between the bulk transformation time and the relaxation time.[14] Jin et al.[15] reported that the density of thin vapor-deposited TPD films can exceed extrapolated undercooled liquid density. Low temperature calorimetric experiments on stable glasses revealed that the density of tunneling states is inversely correlated to degree of stability of the TPD glasses, regardless of their layering and molecular ordering.[16]

These experimental findings provide a way to achieve kinetically inaccessible regions in the energy landscape that are important for understanding the glass transition phenomenon. Tool[17] introduced the first mathematical approach to characterize structural relaxation in glass by defining the fictive temperature, $T_f$, of the glass as the temperature at which the glass structure would be at equilibrium. Probably, the most important contribution is described in Narayanaswamy's seminal paper[18] in which strongly nonlinear structural relaxation is expressed by a linear convolution integral if one replaces the time integration variable by the so-called *material time*. Mazurin et al.[19] and Moynihan et al.[20,21] then combined *nonlinearity* embeded in Tool's fictive temperature and the material-time concept with the stretched exponential function to account for the *nonexponentiality* of the structural relaxation. These features represent the TNM phenomenological model that has been used routinely in industry for decades.[22-24] However, to our knowledge, no attempt has been made to apply this model for the description of the structural relaxation in stable glasses. In this study, the structural relaxation dynamics of previously reported stable and aged TPD thin films[10,11,15] is quantitatively analyzed and described by the TNM model and compared with detailed analysis of conventionally prepared bulk glass of the same chemical composition.

EXPERIMENTAL

The small organic molecule N,N' -Bis(3-methylphenyl)-N,N' - diphenylbenzidine (TPD) was purchased from Sigma-Aldrich (crystalline material, 99.5 % purity) and used without further purification. The amorphous TPD was prepared in two ways. First, a classical melt-quench method was used, based on the melting of the as-purchased crystalline material in a vial in an oil bath: the oil was heated to 453 K (approximately 15 K above the melting temperature of TPD). The vial with the melt was consequently quenched in water, and the obtained glassy TPD ingot was powdered. The second used preparation route was the so-called micro-melt-quench method, where the melting and consequent quenching / cooling were performed directly in the DSC instrument: approximately 2 mg of the crystalline TPD was hermetically sealed in the low-mass Al pan, heated to 453 K to melt the material, and then cooled at 50 $K \cdot min^{-1}$ to 283 K to form the glassy phase. While both preparation routes produced fully amorphous TPD, the powdered material had an increased tendency toward crystallization during the cyclic relaxation experiments. The degradation of the amorphous phase occurred even for very coarse powders (500 – 100 μm diameter fraction), with the crystal growth starting from the mechanically induced defects – sharp edges and microcracks within the grains. On the other hand, the DSC-amorphized TPD was proven to be remarkably stable up to ~ 15 K above $T_g$, with no crystalline phase forming either at the Al-TPD (bottom and side of the DSC pans) interface or at the free surface during the whole experimental procedure. Consequently, only the DSC-amorphized TPD samples were used for the structural relaxation measurements.

The enthalpic manifestation of the structural relaxation process was recorded calorimetrically, using a DSC heat flow instrument (Q2000, TA Instruments) equipped with an autosampler, an RCS90 cooling accessory, and *T*-zero technology. The calibration of the DSC was performed using the In, Zn, and $H_2O$ standards. The relaxation behavior was studied on the basis of two types of temperature-cyclic experiments. As the first type of relaxation measurements, constant heating rate (CHR) cycles[25] were used, where the sample was repeatedly cooled and heated through the glass transition region. Each CHR cycle consists of three steps. The sample was first briefly annealed at the initial temperature $T_{high}$ (well above the glass transition temperature $T_g$, in the undercooled liquid state) to fully erase the previous thermal history and achieve thermo-structural equilibrium. In the second step, the sample is cooled to $T_{low}$, which is well below $T_g$ for the glassy state to be fully reached. In the third step, the sample is immediately heated back to the $T_{high}$. For TPD, the temperature limits for the CHR cycles were set at 283 – 353 K. The upper temperature limit $T_{high}$ had to be iteratively optimized during a preliminary series of measurements because above 353 K, even the DSC-amorphized TPD samples started to exhibit signs of the crystalline phase being formed. The $T_{high}$ = 353 K was found to be optimal with regard to

both, the sample reaching the undercooled liquid equilibrium and not crystallizing during the experiment. The cooling rates applied during the CHR cycles were $q^-$ = 1, 2, 3, 5, 7, 10 and 15 K·min$^{-1}$; the heating rate was for all cycles constant $q^+$ = 30 K·min$^{-1}$.

The second type of relaxation measurements were the peak-shift (PS) four-step cycles.[26] Similarly to the CHR cycles, the PS cycles utilize the equilibration at $T_{high}$ as the first step. In the second step, the sample was cooled at 50 K·min$^{-1}$ to a pre-selected annealing temperature $T_a$ = 318 K (the temperature was, similarly to $T_{high}$, optimized prior to the final set of PS cyclic measurements, so that the relaxation proceeded within a suitable time-frame). In the third step, the sample was annealed at $T_a$ for different annealing times $t_a$ (1, 10, 30, 60, 120, 180, 300, 600, 1200 and 1800 min in the present study). In the fourth step, the sample is heated back to the $T_{high}$ at 10 K·min$^{-1}$. Note that $T_a$ selection of was optimized in a series of tests, so that the relaxation process proceeded reasonably quickly, but not too quickly, for the structural equilibrium to be reached before the occurrence of the so-called 'main peaks'.[26-28]

RESULTS

The most common way of enumerating the TNM parameters is the non-linear optimization of the TNM description of the DSC data. The mathematical modelling of the TNM kinetics is usually based on a numerical algorithm in the form of Eq.(1) for the non-isothermal segments and Eq. 2 for the isothermal segments:

$$T_{f,n} = T_0 + \sum_{j=1}^{n} \Delta T_j \left\{ 1 - \exp\left[ -\left( \sum_{k=j}^{n} \Delta T_k / q_k \tau_k \right)^{\beta} \right] \right\} \quad (1)$$

$$T_{f,n} = T_0 + \sum_{j=1}^{n_A} \Delta T_j \left\{ 1 - \exp\left[ -\left( \sum_{k=n_A}^{n} \Delta t_{e,k} / \tau_k \right)^{\beta} \right] \right\} \quad (2)$$

here $T_0$ is the initial equilibrium temperature, $t_e$ is the annealing time, and $0 < \beta < 1$ is the non-exponentiality parameter, inversely proportional to the width of a distribution of relaxation times. The overarching quantity, the fictive temperature $T_f$, is a way of describing the relaxing structure under any given circumstances either during non-isothermal heating/cooling or during isothermal annealing. It is defined as the temperature at which the measured property (enthalpy or volume) would be equal to the extrapolated equilibrium property. In this way, the fictive temperature practically represents the deviation of the structural state from that of the undercooled liquid; the course of $T_f$ is reminiscent of that for enthalpy or volume but free from the influence of e.g. heat capacity or thermal expansion. The advantage of $T_f$ is its universality (which can be derived for any measured property) and in representing

truly only the relaxation-induced changes, free from the thermo-physical background (e.g. heat capacity or thermal expansion). The relaxation time is defined as

$$\tau = A \cdot \exp\left[ x\frac{h^*/R}{T} + (1-x)\frac{h^*/R}{T_f} \right] \quad (3)$$

where $0 < x \leq 1$ is the nonlinearity parameter, $h^*/R$ is the effective activation energy and $A$ is an adjustable parameter. The fundamental basis of the algorithm is explained in detail in Ref. 29. The $\Delta T$ = 0.1 K (precision 10 times better than suggested in Ref.29) was used for the present calculations. The isothermal segments were divided for modeling purposes into 500 equidistant steps along a logarithmic scale. The consequent nonlinear optimization based on the minimization of the SSR (sum of squared residue) was done using the Levenberg-Marquardt algorithm. The optimization was performed with all four TNM parameters changing freely and simultaneously; only the data corresponding to the heating scans were optimized; each heating scan was optimized separately. In the present study, the DSC data corresponding to the CHR cycles were used (according to Ref.30) as the experimental basis for the nonlinear optimization-based determination of the four TNM parameters. The raw DSC record of the CHR cyclic experiments is shown in Fig. 1.

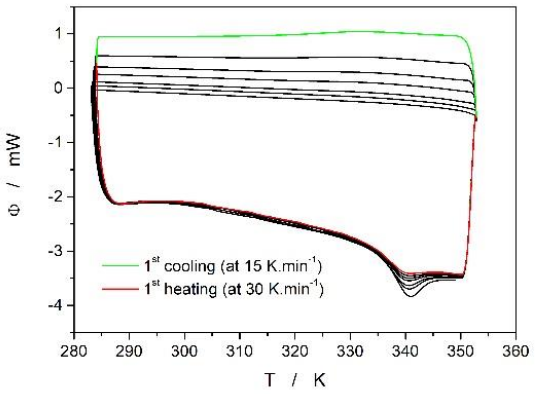


**Fig.1** The set of CHR cyclic relaxation measurement for the bulk TPD glass measured by differential scanning calorimetry. The heating rate for all cycles was $q^+ = 30$ K·min$^{-1}$ and the cooling rates were $q^- = 1, 2, 3, 5, 7, 10$ and 15 K·min$^{-1}$. Exothermic effects evolve in the upward direction.

Note that the DSC signal (apparent baseline) shifts for the different cooling steps as a consequence of the different $q^-$ being used during the CHR cycles; the signal during the heating steps follows a similar baseline due to the usage of an identical/constant $q^+$. In comparison with the literature data[5,13,14] on the annealed highly stable thick and thin TPD films, the relaxation behavior of conventionally prepared bulk TPD glass (data in Fig. 1) is in a very good agreement with the thick 30 µm films annealed 14 K above $T_g$ for ≥ 150 min exhibiting a conventional behavior (note that the data in Ref.5 were measured

at 10 K·min$^{-1}$, while the data in Fig. 1 were measured at 30 K·min$^{-1}$, hence a small increase in $T_g$ and the height of the relaxation peak has to be taken into account). However, the as-deposited ultra-stable 30 μm film exhibited $T_g$ higher by approximately 25 – 30 K and the height of the relaxation peak almost 20 times larger. A significantly smaller proportional change was then observed for the relaxation peak height of the 80 nm thin TPD films, which were however heated at 30000 K·s$^{-1}$, shifting the $T_g$ into the 370 – 430 K region, where the behavior may be different.

Since the temperature dependences of the heat capacities below and above $T_g$ are not similar, and the absolute values of the heat capacities change with the proceeding cycling, the data need to be normalized to separate the pure structural relaxation response from the underlying thermo-physical background (i.e., the courses of the temperature dependences of heat capacities in the glassy and undercooled liquid states):

$$C_p^{red} = \frac{dT_f}{dT} = \frac{\Phi - \Phi_g}{\Phi_l - \Phi_g} \tag{5}$$

where Φ is the measured heat flow, $\Phi_g$ is the extrapolated temperature dependence of the heat flow in the glassy region (stabilized below $T_g$), $\Phi_l$ is the extrapolated temperature dependence of the heat flow in the undercooled liquid region (stabilized above $T_g$), and $C_p^{red}$ is the standard reduced heat capacity signal. The $dT_f/dT$ signal gives the reduced $c_p$ ($c_p^{red}$), similarly as $d\Delta H/dT$ gives $c_p$.[20,21] The normalized CHR cycles data fit by the TNM model is shown in Fig. 2 – the curves obtained at $q^+$ = 10 and 15 K·min$^{-1}$ were omitted from the evaluation due to the increased uncertainty of the fit. The mean SSR for the fits displayed in Fig. 2 was 0.020 ± 0.009.

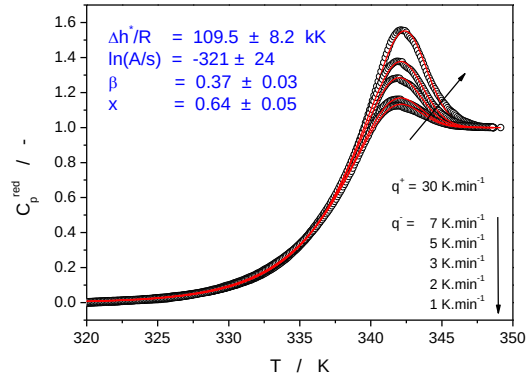


**Fig.2** Normalized heating scans from the low $q^-$ CHR cycles measured for the bulk TPD glass; height of the relaxation peak increases with decreasing $q^-$ (as indicated by the arrows). Points correspond to the experimental data, and solid lines were fitted by the TNM model (for the parameters indicated).

The final set of the TNM parameters obtained for TPD (displayed in Fig. 2) was calculated by averaging the results of each individual optimization performed for the separate heating scans (parameters of

the individual fits are listed in the Supporting information). Whereas certain fits exhibit small systematic deviations, these are rather common (often associated with thermal gradients within the system) and should have no effect on the relaxation results, as the fitting procedure (and the TNM model in general) is most sensitive to the height of the relaxation peak, its half-width and position in temperature. To demonstrate that the undercooled liquid state was reached during all measurements, the $C_p^{red}$-T dependences from Fig. 2 were transformed into the $T_f$-T dependences – see the Supporting information. The full overlap of these data at high temperatures indicates that the undercooled liquid state was reached before each heating step was finished.

Independent confirmation of the curve-fitting results was made by using two well-known linearization approaches (as opposed to the curve-fitting method described above): the Moynihan's[20,21] and Hutchison's[27,28] methods. The Moynihan's linearization method for determination of the apparent activation energy $\Delta h^*$ is based on the dependence of $T_g$ (or the fictive temperature $T_f$) on the cooling rate during the CHR cycles:

$$\frac{d\ln|q^-|}{d(1/T_f)} = -h^*/R \tag{6}$$

where $T_f$ is determined using the equal area method:

$$\int_{T^*}^{T_f}(c_{pl} - c_{pg})dT_f = \int_{T^*}^{T'}(c_p - c_{pg})dT \tag{7}$$

The symbol $T^*$ in Eq.(7) corresponds to any temperature above $T_g$ at which the heat capacity $c_p$ is equal to the equilibrium undercooled liquid value $c_{pl}$, and $T'$ is a temperature well below $T_g$ where a constant glassy value of $c_{pg}$ was achieved.

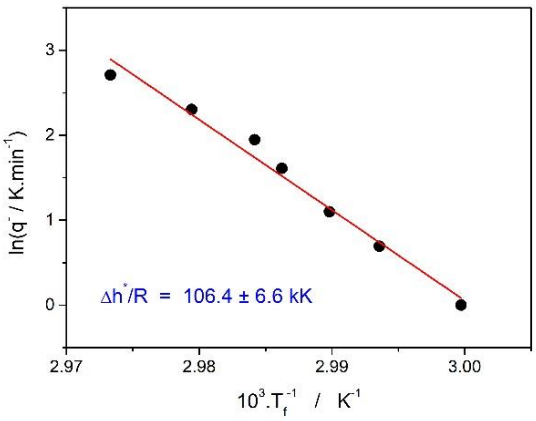


**Fig.3** Determination of the apparent activation energy $h^*$/R according to the Moynihan's method (Eqs. 6 and 7). Points correspond to experimental data and solid line is a linear fit to these data.

The evaluation according to Eq.(6) is for the current CHR cycles data shown in Fig. 3. The calculated value of the apparent activation energy is $h^*/R$ = 106 ± 7 kK. Taking into account the experimental uncertainties, the activation energies determined by the Moynihan linearization method are in a good agreement with those obtained from the non-linear optimization.

The second linearization (non-fitting) method utilized was the Hutchinson peak shift method, where the nonlinearity parameter *x* is evaluated from the four-step peak shift experiments. The PS method is based on the gradual shift of the temperature corresponding to the maximum of the relaxation peak with an increasingly deeper state of relaxation achieved during a gradually prolonged annealing below $T_g$ performed prior to the evaluated heating scan. The state of the relaxation is reflected (similarly to the Moynihan method, i.e., Eq. 7) by means of the excess enthalpy determined from the area under the relaxation peak. In particular, the evaluation is based on the following equation:[28]

$$x^{-1} - 1 = \Delta c_p \left( \frac{\partial T_p}{\partial \delta_H} \right)_{q^-, q^+} \tag{8}$$

where $\delta_H$ is the normalized total excess enthalpy defined as the difference between the excess enthalpy achieved during the cycle when relaxation proceeded and the pseudo-equilibrium enthalpy achieved during the cycle with $t_a$ = 1 ("normalized" indicates the evaluation of the data in $C_p^{red}$ format), $T_p$ is the temperature corresponding to the maximum of the relaxation peak during the fourth peak shift cycle step (the heating scan), and $\Delta c_p$ is the difference between the heat capacities in the undercooled liquid and glass. The application of the peak-shift method to the present TPD bulk data is shown in Fig. 4.

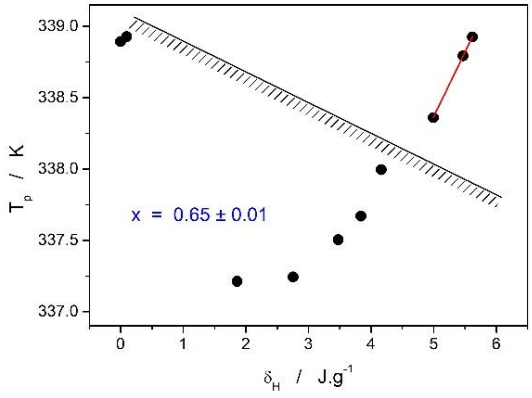


**Fig.4** Determination of x according to the Hutchinson's method. Points correspond to the experimental data, and full line is a linear fit (Eq. 8). The shaded line indicates the approximate region in which the type of peak changes from a main peak (to the right of the shaded line) to so-called 'upper peak', which cannot be used for the evaluation of *x* (Refs. 27 and 28).

According to the theoretical background of the method,[27,28] the slope of the $T_p$-$\delta_H$ dependence must be evaluated only for the 'main' relaxation peaks that occur at sufficiently long relaxation times. For

the present material, this condition was fulfilled for $t_a \geq 600$min, when a linear dependence started to occur in the data. The value of the non-linearity parameter determined according to Eq.(6) is $x \cong 0.65$ assuming that $\Delta c_p = 0.60$ J·K$^{-1}$·g$^{-1}$ (evaluation of $\Delta c_p$ is shown in Supporting information). The $T_p$-$\delta_H$ dependence shown in Fig. 4 is well in agreement with one of the archetypal behaviors identified for different combinations of the β and x TNM parameters, as identified in a recent study[24] of the behavior and errors associated with the peak shift method using theoretically simulated derivative relaxation data (similar to the DSC signal). The present values of β and x (determined independently by means of curve fitting and by the peak shift method) also agree very well with the general prediction based on the identification of this behavior, providing a further mutual consistency between the data and the theory. Considering that the peak-shift method slightly overestimates the true value of *x*, this value is in perfect agreement with the non-linear optimization results.[24]

## DISCUSSION

The dynamics of enthalpy relaxation of conventionally prepared bulk TPD is similar to that of bulk indomethacin[31] prepared in the same way, where a low value of $T_g$ is combined with a relatively large value of the apparent activation energy $h^*/R$ and an intermediate value of the nonexponentiality parameter $\beta$. This combination results in rather slow enthalpy relaxation in these conventionally prepared bulk molecular glasses. It is of interest to compare the relaxation kinetics in a bulk TPD glass presented here with stable vapor-deposited thin film of the same composition. Although, there are some valuable calorimetric studies for TPD thin films,[13,14] reported data do not allow TNM calculations described in previous section. However, Zhang and Fakhraai[11] and recently Jin et al.[15] measured the relaxation behavior of freshly prepared TPD thin films as well as samples aged under well-defined conditions using variable-angle spectroscopic ellipsometry. Points in Fig.5a show the normalized thickness change of a 400 nm TPD thin film equilibrated at 348 K ($T_g$ + 18 K) cooled to 297 K (0.9$T_g$) at -10 K/min (step #1), followed by one week annealing at this temperature (step #2), and then subsequently heated back to 348 K at +10 K/min (step #3).[11] Points in Fig.5b show the normalized thickness change of a 200 nm freshly deposited stable TPD thin film at 0.8$T_g$ monitored during heating at +10 K/min to 348 K (step #1) followed by cooling back at -10 K/min.[15] The full lines in Fig.5 represent the TNM fit to the experimental data (the data were transformed into $T_f$ for the fit, and then re-transformed back into thickness for the visualization in Fig. 5; the set of equations used for the transformation is shown in the Supporting information). The final set of TNM parameters (displayed in Figs.5a and 5b) was calculated by averaging the results of individual optimization performed for the separated steps indicated in Figure 5.

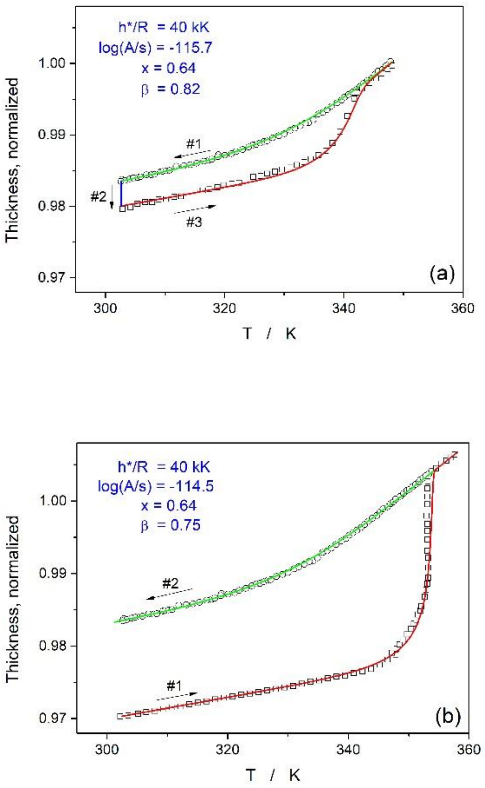


**Fig.5** (a) Thickness change of a 400nm TPD thin film equilibrated at 348 K, cooled to 297 K at -10 K/min (step #1), followed by one week annealing at this temperature (step #2), and then heated to 348 K at +10 K/min (step #3). (b) Thickness change of a 200 nm freshly deposited stable TPD thin film at 264 K heated at +10 K/min to 348 K (step #1) followed by cooling back at -10 K/min. Points correspond to the data reported in Ref. 11 (Fig.1a) and Ref. 15 (Fig.S17a). Full lines are best fits of the TNM model for the parameters indicated.

The apparent activation energy calculated by TNM fits of normalized thickness data sets shown in Fig.5 (h*/R = 40 kK) is more than 60% lower compared with the enthalpy relaxation data of the bulk TPD (see Fig.2). It is well known that when stable glasses are annealed above $T_g$, they lose their thermal stability and transform into the undercooled liquid via a constant velocity propagating fronts. Walters et al.[8] found that while the transformation front velocity varies by over an order of magnitude with $T_{substrate}$, the corresponding activation energy $E_a$ remains constant. They found that the activation energy for the surface initiated front in the 100nm TPD thin film is very similar to that for the substrate initiated front, being about $E_a/R = 45 \pm 4$ kK.[8] This is not so different from the h*/R value found obtained by TNM fits for similar thicknesses of TPD thin films (see Fig.5). Zhang et al.[10] also mentioned that the temperature dependence of the effective viscosity for 100nm thin film matches that of bulk viscosity. This seems to be consistent with the fact that the activation energy of viscous flow is close to the apparent activation energy of structural relaxation for many glass-forming systems.[24]

It should be mentioned that there is a continuing debate as to whether the relaxation kinetics based on the same fictive temperature can be applied to different physical properties. For instance,

DeBolt et al. [21] in their early paper found that glassy $B_2O_3$ exhibits different relaxation kinetics for refractive index and enthalpy. However, more recent investigations have shown that for most inorganic glasses and organic polymers, the enthalpy and volume relaxation kinetics were experimentally indistinguishable within the glass transition region.[24, 32-35] For many glass-forming systems it means that while the magnitude of a change in enthalpy or volume might not be the same, the rate at which each property change within the experimental time scale seems to be similar.[33] In any case, it is of interest to compare relaxation dynamics of different physical properties, taking into account experimental details and entire thermal history of glassy material studied.

Unfortunately, present data do not allow to make such comparison of fictive temperatures derived from different materials properties. Nevertheless, we can discuss isothermal annealing for one week of a 400 nm TPD thin film at $T_a = 0.9T_g$ (step #2 in Fig.5a). Figure 6 shows the entire change in $T_f$ at this temperature calculated for TNM parameters (see Fig.5a) by Eq.(2) and plotted on a logarithmic time scale. It is seen that during the first two hours there is practically no measurable change in $T_f$. It starts to change significantly after approximately 24 hours, reaching maximum rate $(dT_f/d\log t)_i$ at the inflection point (6.29, 317 K), i.e., after about 22 days. The metastable equilibrium at $T_a = 0.9T_g$ would be reached at the extrapolated time $\log(t_m/s) = 8.12$ (approximately 4.2 years). The calculated fictive temperature after 1 week annealing is 322.4 K that is nearly identical to the $T_f = 322.6$ K reported by Zhang and Fakhraai.[11]

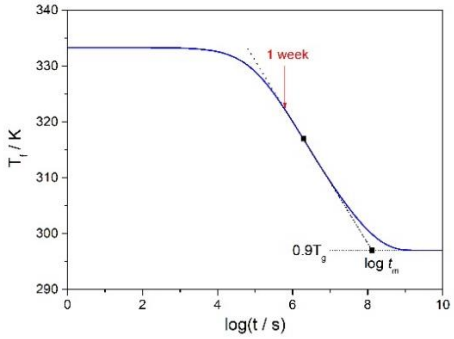


**Fig.6** Time evolution of the fictive temperature of a 400 nm TPD thin film (Ref.11) at $T_a = 0.9T_g$ calculated by Eq.(2). The dashed line corresponds to the inflection tangent. The arrow indicates $T_f$ after 1 week of annealing (step #2 in Fig.5a).

As the extrapolated value of $\log(t_m/s)$ is relatively close to equilibrium, it is possible to neglect nonlinearity and nonexponentiality effects and we can assume nearly linear change of $\log t_m$ with the annealing temperature:[36]

$$\frac{d\log t_m}{d(1/T_a)} \cong \frac{h^*/R}{2.303} \qquad (9)$$

where $h^*/R$ is identical to the apparent activation energy obtained from the cooling scans. The full lines in Fig.7 shows the prediction of Eq.(9) assuming that $t_m$ = 100s at $T_g$.

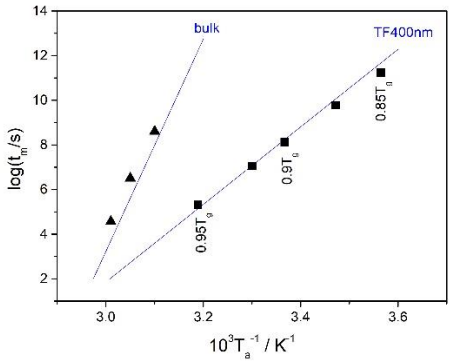


**Fig.7** The extrapolated equilibrium relaxation time estimated by Eq.(9) as a function of $1/T_a$ for conventionally prepared TPD bulk glass and stable thin film (solid lines). Points were calculated by Eq.(2) for the TNM parameters corresponding to bulk glass (Fig.2) and 400nm aged thin film (Fig.5a).

The points were determined by extrapolating the inflection tangent to the $T_f(\log t)$ curves calculated by Eq.(2) for the TNM parameters corresponding to the bulk TPD glass (Fig.2) and the 400nm TPD thin film (Fig.5a). We can roughly estimate that the time needed to reach equilibrium for 400nm aged TPD thin film at temperature $T_a = 0.85T_g$ is about 5400 years. In contrast, approximately same time would be needed for a conventionally prepared bulk glass much closer to the glass transition temperature ($T_a = 0.94T_g$).

The activation energy of structural relaxation is an important parameter characterizing the dynamics of structural change during cooling ramp from temperatures above $T_g$ or isothermal physical aging close to a metastable equilibrium because under such conditions the nonlinearity and nonexponentiality contributions are negligible. However, these two essential aspects of the structural relaxation should be known for any prediction of the relaxation rate. Recently, Málek[37,38] has shown that the relaxation rate expressed as the fictive temperature change per decade of time $R_{10} = (dT_f/d\log t)_i$ at 10 K below $T_g$ can be used as a convenient scale to compare the relaxation dynamics in many different glass-formers. It can be expressed as[37,38]

$$R_{10} \cong \left[\frac{0.118}{\beta} + \frac{\sigma}{2.303}\right]^{-1} \qquad (10)$$

where $\beta$ is the nonexponentiality parameter characterizing the distribution of relaxation times and the parameter $\sigma$ quantifies overall nonlinearity. This parameter expresses a partial derivative of logarithm of the relaxation time with respect to the fictive temperature at the inflection point of the isothermal relaxation curve, i.e. $\sigma = -(\partial \ln\tau/\partial T_f)_i$. It is defined for the TNM model as:[36-38]

$$\sigma \cong (1-x)\cdot \frac{h^* / R}{T_g^2} \qquad (11)$$

involving the effective activation energy $h^*/R$, the nonlinearity parameter $x$, and the glass transition temperature $T_g$. It should be pointed out that the nonexponentiality and nonlinearity expressions are clearly separated in Eq.(11), even though they seem to be inextricably bound together by the material time.[24,33,39]

Figure 8 shows the $R_{10}$ plotted as a function of the parameter $\sigma$. Solid blue lines were calculated by Eq.(10) for constant values of the nonexponentiality parameter $0.2 \le \beta \le 0.8$. The maximum relaxation rate (8.5 K/decade) can be expected for purely exponential relaxation ($\beta = 1$) and $\sigma = 0$ K$^{-1}$. The structural relaxation rate $R_{10}$ of any amorphous material at $T_g$-10 should be within a scale bounded by this upper limit of the relative change of $T_f$ per decade of time. Therefore, $R_{10}$ has been proposed as a scale to compare the structural relaxation rate of amorphous materials at $T_a = T_g$-10.[37,38]

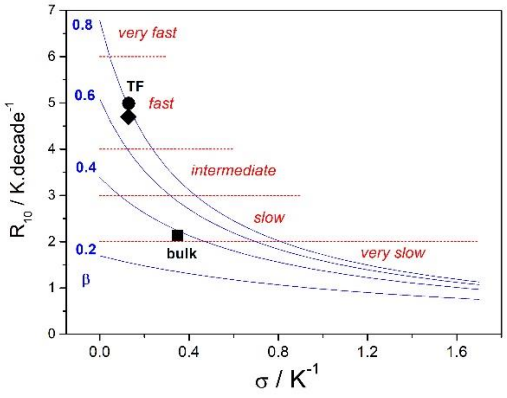


**Fig.8** Relaxation rate at $T_a = T_g$-10 as a function of nonlinearity contribution $\sigma$. Solid lines were calculated by Eq.(10) for constant values of the parameter $\beta$ indicated next to the curves. The dashed lines indicate five ranges of the structural relaxation rate (Ref.38). The points correspond to the relaxation of bulk TPD glass ■ (this paper), 200nm stable thin film ◆ (Ref.15, Fig.S17a) and 400nm aged thin film ● (Ref.11, Fig.1a) of the same composition.

This relaxation rate scale can be subdivided into five distinct rate ranges (red dashed lines in Fig.8): very fast relaxation $5 < R_{10} < 8.5$, fast relaxation $4 < R_{10} \le 5$, intermediate relaxation $3 < R_{10} \le 4$, slow relaxation $2 < R_{10} \le 3$ and very slow relaxation $R_{10} \le 2$ K/decade of time. Now we can compare the relaxation rate in conventionally prepared bulk, stable, and aged TPD glass. The parameter $\sigma$ is calculated by Eq.(11) where $T_g$ is set for the relaxation time $\tau = 100$ s in equilibrium ($T_f = T$). Then, for the TNM model follows from Eq.(3): $T_g \cong (h^*/R)/(\ln 100 - \ln A)$. Using the TNM parameters (shown in Figs.2 and 5) we get $\sigma = 0.349$ K$^{-1}$ for the conventional bulk TPD glass, $\sigma = 0.128$ K$^{-1}$ for stable thin film (200 nm), and $\sigma = 0.130$ K$^{-1}$ for aged thin film (400 nm) of the same composition. The relaxation rate $R_{10}$ calculated by Eq.(10) is then plotted in Fig.8. It is seen that there is a significant difference in relaxation rate. Although the

conventional bulk TPD glass approaches very slow relaxation range, the stable thin film (prepared by PVD) exhibit fast relaxation, which is comparable to some metallic, silicate or chalcogenide glasses.[38] It is interesting that similarly fast relaxation rate is expected also for aged thin film where the previous thermal history has been erased before aging.

Considering that the parameter $\sigma$ is for the thin films nearly three times lower and the parameter $\beta$ is more than two times higher compared to the bulk material, it is clear that the variety of the relaxation motions (represented by $\beta$) has for the TPD material a dominant influence over the relaxation rate $R_{10}$. Note that the dominance of the $\beta$ contribution is characteristic only for the low-$\sigma$ relaxation processes that generally exhibit higher relaxation rates – as implied from Fig. 8. In this relaxation regime, it is, therefore, worth considering the possible structural explanation for such high difference in the variety of the employed relaxation motions (the variety being significantly lower for the thin films compared to their bulk counterpart). In this regard, the key aspect may be associated with the successful predictions[13,14] of the glass→undercooled liquid transformation in stable thin films in terms of the facilitated kinetic Ising models. According to this concept, the structural relaxation transition happens along the narrow front propagating through the thin film (usually from the free surface, i.e., the region with highest mobility, to the substrate). Due to the nature of this propagation, it is possible that only certain relaxation motions can in the spatially restricted and anisotropic environment participate in the overall relaxation response; hence, the narrower distribution of the relaxation times. Akin limitation evidently occurs also for the long-aged thin TPD film (see Fig. 5a), which imposes a question of whether a similarly anisotropic molecular structure (with gradient in mobility) naturally forms also during the relaxation of the annealed thin film with already erased initial thermal history associated with the deposition. Despite the much smaller extent of the equilibrium relaxation packing being expected for the annealed thin film (compared to the as-deposited one), the state of the one-week-annealed structure is still very far from equilibrium (Fig. 6), which further conforms with the idea of the anisotropicity being introduced into the thin film either via the depth gradient of the relaxation rate itself or through a secondary structural loosening through the surface self-diffusion.

## CONCLUSIONS

The structural relaxation dynamics of previously reported TPD thin film stable[11] and aged glasses[15] is quantitatively described by the TNM model and compared with a detailed analysis of conventionally prepared bulk glass of the same chemical composition. A significantly higher nonexponentiality parameter ($\beta \approx 0.8$) found for stable and aged thin films reveals a narrower

distribution of relaxation times in comparison with the conventional bulk glass ($\beta \approx 0.4$). Nearly three times lower value of the overall nonlinearity parameter ($\sigma \approx 0.13$) for stable thin films indicates weaker dependence of the average relaxation time on structural changes (i.e. the fictive temperature dependence) than observed in conventional bulk glass. The apparent activation energy calculated by TNM fits of normalized thickness data[11,15] is close to the activation energy for the surface and substrate initiated front in the 100nm TPD thin film ($h^*/R = 45 \pm 4$ kK) reported by Walters et al.[8]

Berthier and Ediger[40] formulated an interesting and provocative question: 'How to measure a structural relaxation time that is too long to be measured?' Although we agree that there is no definitive answer to this question, we hope that the simple methods presented here (based on the TNM phenomenology) could provide a useful tool for an estimation of the time scale and rate of structural relaxation in stable and aged thin film materials prepared by PVD. Especially, the measurement of cooling-rate-dependent $T_g$ and aging experiments monitored by ellipsometry seems to be useful in this respect. Based on the TMN analysis we can estimate that the time needed to reach equilibrium for 400nm TPD thin film is about 5 400 years at temperature $0.85T_g$. In contrast, it would take approximately same time much closer to the glass transition temperature ($0.94T_g$) for a conventionally prepared bulk glass. The structural relaxation of these promising stable materials can be controlled by the substrate temperature, deposition rate, the chemical composition of a glassformer as well as by physical aging. Their fine-tuning improves the quantum efficiency and lifetime of light-emitting diodes and other organic electronic devices.[41] A better understanding of the relaxation dynamics in stable thin films as well as the surface-mediated aging can help to develop a predictive understanding of the stable glass-forming materials.[42]

## SUPPLEMENTARY MATERIAL

See the supplementary material for detailed information about the curve fitting procedure applied to constant heating rate (CHR) cycles of conventionally prepared bulk TPD glass (Table S1, Fig.S1), determination the $\Delta c_p$ value from DSC data (Fig.S2), and more details about transformation of thickness data into $T_f$.


## ACKNOWLEDGMENTS

This work was supported by the Selected Research Teams Program of the Faculty of Chemical Technology, University of Pardubice. The author expresses thanks to Prof. Pavel Čičmanec for his invaluable help with the development of a computer program for modelling the structural relaxation.

REFERENCES


1. S.F. Swallen., K.L. Kearns, M.K. Mapes, Y.S, Kim, R,J. McMahon, M.D. Ediger, T, Wu, L. Yu, S. Satija, Science **315**, 353 (2007).
2. M.D. Ediger, J. Chem. Phys. **147**, 210901 (2017).
3. M.D. Ediger, J. De Pablo, L. Yu, Acc. Chem. Res. **52**, 407 (2019).
4. K. Bagchi, M.D. Ediger, J. Phys. Chem. Lett. **11**, 6935 (2020).
5. C. Rodríguez-Tinoco, M. Gonzalez-Silveira, M.A. Ramos, J. Rogriguez-Viejo, Rivista del Nuovo Cimento **45**, 325 (2022).
6. S.S. Dalal, D.M. Walters, I. Lyubimov, J. De Pablo, M.D. Ediger, Proc. Natl. Acad. Sci. **112**, 4227 (2015).
7. A. Gujral, K.A. O'Hara, M.F Toney, M.L. Chabinyc, M.L., M.D. Ediger, Chem. Mater. **27**, 3341 (2015).
8. D.M. Walters, R. Richert, M.D. Ediger, J. Chem. Phys. **142**, 134504 (2015).
9. Y. Zhang, R. Potter, W. Zhang, Z. Fakhraai, Soft Matter. **12**, 9115 (2016).
10. Y. Zhang, E.C. Glor, M. Li, T. Liu, K. Wahid, W. Zhang, R.A. Riggleman, Z. Fakhraai, J. Chem. Phys. **145**, 114502 (2016).
11. Y. Zhang, Z. Fakhraai, Phys. Rev. Lett. **118**, 066101 (2017).
12. J. Ráfols-Ribé, R. Dettori, P. Ferrando-Villalba, M. Gonzalez-Silveira, L. Abad, A.F. Lopeandía, Colombo, J. Rodríguez-Viejo, Phys. Rev. Mater. **2**, 035603 (2018).
13. J. Ráfols-Ribé, A. Vila-Costa, C. Rodríguez-Tinoco, A.F. Lopeandía, J. Rodríguez-Viejo, M. Gonzalez-Silveira, Phys. Chem. Chem. Phys. **20**, 29989 (2018).
14. C. Rodríguez-Tinoco, M. Gonzalez-Silveira, J. Ráfols-Ribé, A. Vila-Costa, J.C. Marinez-Garcia, J.Rogríguez-Viejo, Phys. Rev. Lett. **123**, 155501 (2019).
15. Y. Jin, A. Zhang, S.E. Wolf, S.Govind, A.R. Moore, M, Zhernenkov, G. Freychet, A.A. Shamsabadi, Z. Fakhraai, Proc. Natl. Acad. Sci. **118**, e2100738118 (2021).
16. M. Moratalla, M. Rodríquez-López, C. Rodríguez-Tinoco, J. Rogríguez-Viejo, R.J. Jiménez-Riobóo; M.A. Ramos, Communications Physics **6**, 274 (2023).
17. A.Q. Tool, J. Am. Ceram. Soc. **29**, 240 (1946).
18. O.S. Narayanaswamy, J. Am. Ceram. Soc. **54,** 491 (1971).
19. O.V. Mazurin, S.M. Rekhson, Y.K. Startsev, Fiz. Khim. Stekla. **1**, 412 (1975). English transl.
20. C.T. Moynihan, A.J. Easteal, M.A. DeBolt, J. Tucker, J. Am. Ceram. Soc. **59**, 12 (1976).
21. M.A. DeBolt, A.J. Easteal, P.B. Macedo, C.T. Moynihan, J. Am. Ceram. Soc. **59**,16 (1976).
22. G. W. Scherer, Relaxation in Glass and Composites, Wiley, New-York (1986).
23. S. Gaylord, B. Ananthasayanam, B. Tincher, L.Petit, C. Cox, U. Fotterningham, P. Joseph, K. Richardson, J. Am. Ceram. Soc. **93**, 220 (2010).
24. I.M. Hodge, J. Non-Cryst. Solids. **169**, 211 (1994).
25. R. Svoboda, J. Non-Cryst. Solids **408**, 115 (2015).
26. R. Svoboda, J. Am. Ceram. Soc. **106**, 5233 (2023).
27. J.M. Hutchinson, A.J. Kovacs, Polym. Eng. Sci. **24**, 1087 (1984).
28. J. M. Hutchinson, M. Ruddy, J. Polym. Sci. B 26, 2341 (1988).
29. I.M. Hodge, A.R. Berens, Macromolecules **15**, 762 (1982).
30. R. Svoboda, J. Málek, J. Non-Cryst. Solids **378**, 185 (2023).
31. R. Svoboda, D. Koštálová, M. Krbal, A. Komersová, Molecules **27**, 5668 (2022).
32. J. Málek, S. Montserrat, Thermochim. Acta **313**, 191 (1998).
33. J. Málek, Macromolecules **31**, 8312 (1998).
34. A. Sipp, P. Richet, J. Non-Cryst. Solids **298**, 202 (2002).
35. U. Fotheringham, A. Baltes, P. Fischer, P. Hohn, R. Jedamzik, C. Schenk, C. Stolz, G. Westenberger, J. Am. Ceram. Soc. **91**, 780 (2008).
36. J. Málek, Thermochim. Acta **313**, 181 (1998).
37. J. Málek, J. Am. Ceram. Soc. **106**, 1739 (2023).
38. J. Málek, J. Phys. Chem. C **127**, 6080 (2023).
39. J.M. Hutchinson, Prog. Polym. Sci. **20**, 703 (1995).
40. L. Berthier, M.D. Ediger, J. Chem. Phys. **153**, 044501 (2020).
41. K. Bagchi, M.D. Ediger, J. Phys. Chem. Lett. **11**, 6935-6945 (2020).
42. P. Luo, Z. Fakhraai, Annu. Rev. Phys. Chem. **74**, 361 (2023).